Connectivity of phases and growth mechanisms in peritectic alloys solidified at low speed: An X-ray tomography study of Cu-Sn

M. Rappaz [a,*], F. Kohler [a], J. Valloton [a], A.B. Phillion [a], and M. Stampanoni [b]

[a] *Computational Materials Laboratory, Ecole Polytechnique Fédérale de Lausanne, Station 12, CH-1015 Lausanne, Switzerland*

[b] *Paul Scherrer Institut, Swiss Light Source, WLGA/135, CH-5323 Villigen, Switzerland*

* Corresponding author. Tel.: ++41 (0)21 693 2844. Fax:++41 (0)21 693 5890. E-mail: michel.rappaz@epfl.ch (M. Rappaz)

Preprint submitted to Nature Materials *19 August 2009*

Abstract

The variety of microstructures that form at low solidification speed in peritectic alloys, -bands, islands or even coupled (or cooperative) growth of the primary $\alpha-$ and peritectic $\beta-$phases-, have been previously explained by nucleation-growth mechanisms. In a recent investigation on Cu-Sn, a new growth mechanism was conjectured on the basis of 2-dimensional optical microscopy and Electron Back-Scattered Diffraction (EBSD) observations made in longitudinal sections. In the present contribution, X-ray tomography has been used to confirm this mechanism: $\alpha-$ and $\beta-$phases can be totally interconnected in 3 dimensions and bands (or islands) can result from an overlay mechanism, rather than from a nucleation events sequence. When the lateral growth of a new layer is too fast, an instability can lead to the formation of a lamellar structure as for eutectic alloys.

Steel, bronze, brass and many other commercially important alloys exhibit peritectic transitions during solidification [1]. This invariant reaction in binary alloys is characterized by the transformation of two phases, liquid (ℓ) and primary phase (α), into the peritectic phase (β), at temperature T_p and peritectic composition C_p (see Fig. 1). In the hypo-peritectic region, i.e., for a nominal composition of the alloy C_0 such that $C_\alpha < C_0 < C_p$, a number of different microstructures have been observed during directional solidification at low growth rate in an imposed thermal gradient G [2]. By low growth rate, we mean a growth velocity V such that a planar front of the α-phase would be stable, should the peritectic phase not be present. This condition is met

when

$$V < V_{crit} = \frac{GD_\ell}{\Delta T_{0\alpha}} \tag{1}$$

where G is the thermal gradient, D_ℓ is the diffusion coefficient of the solute element in the liquid phase and $\Delta T_{0\alpha}$ the solidification interval of the α-phase.

[Fig. 1 about here.]

The diversity of microstructures obtained when $C_\alpha < C_0 < C_p$ and $V < V_{crit}$ is due to an inherent instability of both the α- and the β-planar fronts. Figure 1 illustrates schematically why neither of these phases are stable under such conditions. Neglecting any nucleation undercooling, the first solid to form under directional solidification is α with a composition $k_{0\alpha}C_0$, where $k_{0\alpha}$ is the partition coefficient for the α phase. In the transient to steady-state, the α-solid grows with a planar front morphology while the interfacial liquid composition $C_\ell^{*\alpha}$ increases from C_0 to $C_0/k_{0\alpha}$ (points labeled (1) to (3) in Fig. 1). Concurrently, the interface temperature moves from the liquidus, $T_{liq}^{\alpha}(C_0)$, to the solidus of α, $T_{sol}^{\alpha}(C_0) = T_{liq}^{\alpha}(C_0/k_{0\alpha})$. However, as soon as $C_\ell^{*\alpha}$ goes beyond $C_\ell = C_\ell(T_p)$, the liquid becomes undercooled with respect to β (grey area in Fig. 1(a)), since the liquidus of α is below that of β. Therefore, the peritectic phase can nucleate and grow ahead of the primary phase [3–5]. If the β-phase entirely covers the primary phase and prevents it from further growth, this gives rise to a *band* of β covering the previous α solid.

Considering now the growth of a β-planar front starting at point (4) (Fig. 1(b)), the solid composition C_β^* is larger than C_0. Therefore, the interfacial composition has to decrease in order to reach a steady-state β-planar front growth (points (4) to (5)). At some point, the liquid interfacial composition falls below $C_\ell(T_p)$. This liquid is now undercooled with respect to α (grey area in Fig.

1(b)), allowing then the α-phase to nucleate and grow ahead of the β phase (point labeled (6)). As the loop shown in Fig. 1 (points (1) to (6)) can start again, this sequence of α- and β-phases nucleation-growth events leads to an alternation of α- and β- bands perpendicular to the thermal gradient G.

Such bands have been observed in longitudinal sections of Fe-Ni alloys [3,12], and more recently in the Cu-Sn system [13]. A Nucleation and Constitutional Undercooling (NCU) criterion has also been developed, by Hunziker *et al* [14], to predict the appearance of these bands based on the critical undercoolings for the nucleation of the α- and β-phases. However, when the lateral spreading of a new phase in a direction perpendicular to G over the pre-existing front growing in the direction of G is considered, together with the solute field interactions near the triple junction $\alpha - \ell - \beta$ [7,5,10], incomplete coverage of one phase over the other may occur. This leads to the formation of *islands*, which are therefore like incomplete bands.

Finally, another interesting microstructure that can form in peritectic alloys at low growth rate is the simultaneous growth of α- and β-lamellae in the direction of the thermal gradient G. Although similar to the well-known coupled growth of eutectic alloys, the α- and β-lamellae of peritectic alloys both reject solute elements ahead of the interface. Less solute is rejected by the β-phase since $k_{0\beta} > k_{0\alpha}$. Predicted in 1959 by Chalmers [16], coupled (or cooperative) growth in peritectic alloys was first observed in Ni-Al, by Lee and Verhoeven [18], and then in Fe-Ni by Kurz and co-workers [19,12]. As shown by directional solidification experiments and multi-phase field simulations [9–12,20], lamellae structures can start growing from islands, providing the distance separating the islands falls within a range of stable lamellar spacings [10].

The observations of bands, islands and cooperative lamellae growth in peritectics was limited up to now to small solidification interval alloys, typically with $\Delta T_{0\alpha} \lesssim 10$ K. Surprisingly, none of the previous investigations tried to determine if the bands, islands and lamellae of the two phases had a crystallographic relationships, e.g., by using Electron Back-Scattered Diffraction (EBSD). In a recent contribution, Kohler *et al*[13] investigated peritectic solidification in the Cu-Sn system, an alloy with a solidification interval $\Delta T_{0\alpha}$ nearly fifty times that of Fe-Ni in the hypo-peritectic region (around 120 K near C_p). Using a Bridgman solidification setup with quench, in which solutal convection was minimized by having small specimen dimensions, these authors observed all three of the peritectic microstructures discussed above - lamellae, bands, and islands. The crystallographic orientations of the resulting microstructures were also investigated.

An example micrograph from the work of Kohler *et al*[13] is shown in Fig. 2 for a Cu-21wt%Sn specimen solidified at 0.58 μm/s. In the top view of this longitudinal section micrograph, the α-phase appears in light brown while the β-phase is colored in blueish brown. The solidification direction goes from left to right. As can be seen, there is a transition in growth from lamellae to bands and then back to lamellae. The transition from bands to lamellae on the right-hand side clearly goes through an intermediate stage of semi-continuity and then partial bands or islands. In the bottom view, a reconstructed false color micrograph obtained from the EBSD measurements is shown. Due to a solid-state transformation of β either into $(\delta + \alpha)$ via a eutectoid reaction or into a martensitic phase, only the α-phase could be indexed. As can be seen, the α-phase in this section is made of two grains, yellow and blue. More importantly, within a grain, the same orientation is measured for the lamellae

on the left and the right sides of the micrograph, and is not lost when discrete bands form in the middle of the longitudinal section.

[Fig. 2 about here.]

These observations can be explained by one of two mechanisms: (i) The whole structure is in fact continuous in 3 dimensions (3D) but may appear as discontinuous discrete bands in 2D metallographic sections; (ii) When a new phase nucleates ahead of an existing one, there is a systematic coherency relationship. Of these two mechanisms, the second mechanism can be immediately ruled out, although a Kurdjumov-Sachs crystallographic relationship was observed between the fcc-α and bcc-β phases in another region of the specimen where the β-phase did not transform and could be indexed [13]. There are 24 such relationships between the $\langle 100 \rangle_\alpha$ and $\langle 100 \rangle_\beta$ reference systems. In the first mechanism, a new band of a phase, say β, does not require any nucleation event at the $\alpha - \ell$ interface if it exists already in another region of the specimen. The new phase β can then simply grow laterally from this region since the liquid ahead of the $\alpha - \ell$ exhibits the largest supersaturation. This "*overgrowth*" or "*overlay" mechanism*, which is of course not possible in 2D, is shown schematically in Fig. 3. As lateral growth of one phase over the other occurs in a nearly nil (horizontal) thermal gradient and at a velocity which can be much higher than the pulling velocity V of the specimen, it can be unstable (see Fig. 3). It then develops β-cells. Since the α-phase is still growing in between the spaces left by the β-cells, an alternate sequence of the primary and peritectic phases is formed and a cooperative growth is thus initiated between the α- and β-phases leading to the formation of a α-β lamellar structure. A similar situation can occur during the lateral propagation of an α-layer over a β-liquid interface. This mechanism is similar to that observed by Akamatsu

125 *et al* [21] on organic eutectic alloys at the onset of coupled growth.

126 [Fig. 3 about here.]

127 In order to check the continuity of the α- and β-phases in 3D, and hence the
128 validity of this growth mechanism, X-ray tomography experiments were car-
129 ried out at the TOMCAT beam-line of the Swiss Light Source (Paul Scherrer
130 Institute, Villigen, Switzerland) on Cu-Sn specimens 300 μm in thickness. The
131 energy of the X-ray beam was 30 keV, the detector resolution was 1.4 μm per
132 voxel side, and the specimen-to-screen distance was 2 mm. The combination
133 of high X-ray energy and small sample dimensions was necessary since both
134 Cu and Sn are strong X-ray absorbers, with Sn having a higher Z-number and
135 hence is more absorbing.

136 Figure 4 shows eight 3D views of the microstructure from a sub-section of
137 the specimen shown in Fig. 2, in a region where lateral overgrowth gave rise
138 to the lamellar structure. The images are shown in reverse contract with the
139 α-phase appears in dark brown since it is leaner in Sn ($C_\alpha \approx 13.5$ wt%), while
140 the β-phase appears brighter since $C_\beta \approx 22$ wt%. In this series of images, the
141 thermal gradient G is vertical; the evolution in microstructure is shown by two
142 fixed vertical sections and one horizontal section which "moves" in the solid-
143 ification direction from image (a) to image (h). Although this sequence was
144 recorded post-mortem, and not in-situ during growth of the microstructure,
145 it shows the complexity of the phase interconnections. In some regions, e.g.,
146 at mid-height, the two longitudinal sections exhibit a band-type morphology.
147 In others, e.g., near the top of the left section, it is clearly lamellar. As shown
148 by the moving horizontal section, the α-phase is interconnected. While lateral
149 growth of both phases appears to be not as smoothed as illustrated in Fig. 3,

it finally gives rise to a fairly regular arrangement of lamellae near the top of the specimen. As mentioned in [13,22], solutal convection is probably responsible for the irregularities of the microstructure, especially during overgrowth. Convection not only gradually increases the average composition of the liquid during growth, due to macrosegregation, it also affects the local composition. Numerical simulations [22] revealed a complex, unsteady streamline pattern, with solute-enriched and solute-lean plumes of liquid going upward and downward, respectively, with a non-zero horizontal component of the velocity (i.e, helicoidal movements).

[Fig. 4 about here.]

The connectivity of the phases can also be seen in the 3D image shown in Figure 5. In this figure, the α phase has been removed from the drawing, leaving only the interconnected β phase. The thermal gradient G is vertical and points up. As can be seen in the figure, the β phase goes through two distinct transitions. Firstly, in the lower half of the image there is a transition from a lamellae to a bands -type structure. Secondly, in the upper half of the image, there is the reverse transition, from a bands to a lamellae -type structure. These transitions, 3D in nature, provide clear evidence supporting the growth overlay mechanism as a means of phase propagation. Although it might appear that the upper β region is separate from the lower region, and hence the result of a new nucleation event, we believe that the two regions are in fact continuous and that the link between these two regions occurs outside the bounding box of the X-ray tomographic scan.

[Fig. 5 about here.]

Despite convection effects and solid state transformations that make the analy-

sis of the post-mortem microstructure more difficult, X-ray tomographic observations have clearly shown the 3D connectivity of the α- and β-phases during low speed growth of Cu-Sn alloys. These observations explain the continuity of the grains measured previously by EBSD in 2D sections and confirm that bands might form by an overgrowth mechanism of one phase over the other and do not require necessarily re-nucleation. If lateral growth is unstable, bands can give rise to lamellae in a similar fashion to the initial state of coupled eutectic growth. X-ray tomography also opens new opportunities for the study of peritectic solidification at low growth rate. In a first step, we plan to grow Cu-Sn alloys in capillaries of smaller dimensions (typically about 400 μm diameter) in order to further reduce convection and allow for 3D characterization of the whole specimen. In a second step, we hope to perform direct in-situ X-ray tomography observations of Cu-Sn growth at low speed in a specifically designed furnace.

1 Acknowledgements

The authors would like to thank the European Spatial Agency (ESA MAP-project AO 98/99-114, ESTEC contract # 14243/00/NL/SH), the Swiss National Fund (contract # 200020-121598), the Natural Sciences and Engineering Research Council (NSERC, Canada) and the Paul Scherrer Institute (proposal #20080240) for their financial and technical support.

References

[1] H.W. Kerr and W. Kurz, Int. Metal Rev. 1996;**41**: 129-164.

[2] W.J. Boettinger, S.R. Coriell, A.L. Greer, A. Karma, W. Kurz, M. Rappaz, and R. Trivedi, Acta Mater. 2000;**48**: 43-70.

[3] R. Trivedi, Metall. Mater. Trans. 1995;**26A**: 1583-1590.

[4] R. Trivedi, H. Miyahara, P. Mazumder, E. Simsek and S.N. Tewari, J. Cryst. Growth 2001;**222**: 365-379.

[5] R. Trivedi and J.S. Park, J. Cryst. Growth 2002;**235**: 572-588.

[6] W.J. Boettinger, Metall. Mater. Trans. 1974;**5**: 2023-2031.

[7] R. Trivedi, A. Karma, T.S. Lo, J.S. Park and M. Plapp. Dynamic pattern formation in the two phase region of peritectic systems. In: Solidification microstructures, Proc. 2nd Workshop Zermatt, 1998.

[8] K. Tokieda, H. Yasuda and I. Ohnaka, Formation of banded structure in Pb-Bi peritectic alloys, 1999, Mater. Sci. Eng. **A**, 238-245.

[9] S. Dobler: Solidification biphasée des alliages péritectiques Fe-Ni, Ecole Polytechnique Fédérale de Lausanne, These 2409, Switzerland, 2001.

[10] T.S. Lo, S. Dobler, M. Plapp, A. Karma and W. Kurz, Acta Mater. 2003;**51**: 599-611.

[11] S. Dobler and W. Kurz, Z.Metallkd.;**95**: 592-595.

[12] S. Dobler, T.S. Lo, M. Plapp, A. Karma and W. Kurz, Acta Mater. 2004;**52**: 2795-2808.

[13] F. Kohler, L. Germond, J.-D. Wagnière and M. Rappaz, Acta. Mater. 2008;**57**: 56-68.

[14] O. Hunziker, M. Vandyoussefi and W. Kurz, Acta Materialia 1998;**46**: 6325-6336.

[15] R. Trivedi, Scripta Mater. 2005;**53**: 47-52.

[16] B. Chalmers: Physical metallurgy. New-York, Wiley, 1959.

[17] M.C. Flemings: Solidification processing. New-York, McGraw-Hill, 1974.

[18] J.H. Lee and J.D. Verhoeven, J. Cryst. Growth 1994;**144**: 353-366.

[19] M. Vandyoussefi, H.W. Kerr and W. Kurz, Acta Mater. 2000;**48**: 2297-2306.

[20] T.S. Lo, A. Karma and M. Plapp: Phase-field modeling of microstructural pattern formation during directional solidification of peritectic alloys without morphological instability, 2001.

[21] S. Akamatsu, S. Moulinet and G. Faivre, Met. Mater. Trans. 2001;**32A**: 2039-2048.

[22] F. Kohler: Peritectic solidification of Cu-Sn alloys: microstructure competition at low speed, Ecole Polytechnique Fédérale de Lausanne, Thesis 4037 (http://library.epfl.ch/theses/?nr=4037), Switzerland, 2008.

[23] J. A. Dantzig and M. Rappaz: *Solidification* (EPFL-Press, Lausanne, Switzerland, 2009).

List of Figures

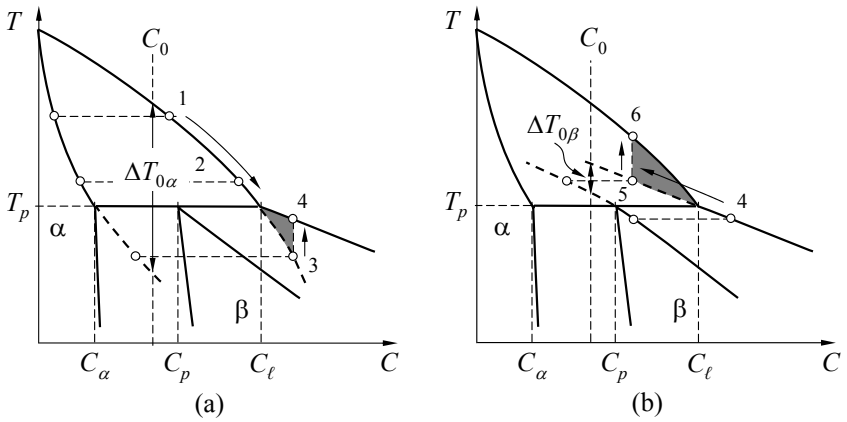

Fig. 1. Schematic diagram of (a) α-planar front growth leading to an undercooled liquid with respect to the β-phase, and (b) β-planar front growth leading to an undercooled liquid with respect to the α-phase.

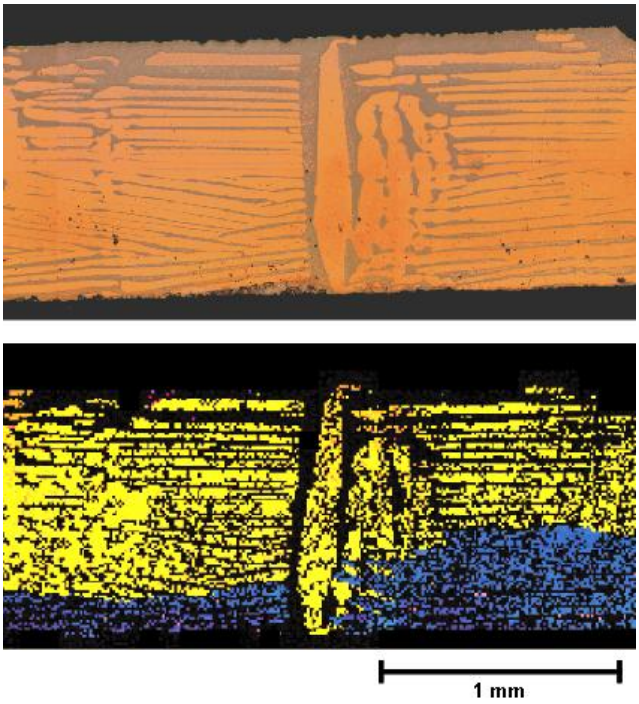

Fig. 2. Longitudinal section of a Cu-21wt%Sn specimen solidified at $V = 0.58$ μm/s in a thermal gradient $G = 200$ K/cm. The top view shows the microstructure with α and β in light brown and blueish brown, respectively. The bottom view shows an EBSD false color reconstructured map based on points measured in the α-phase. (Enlarge view from [13,22]).

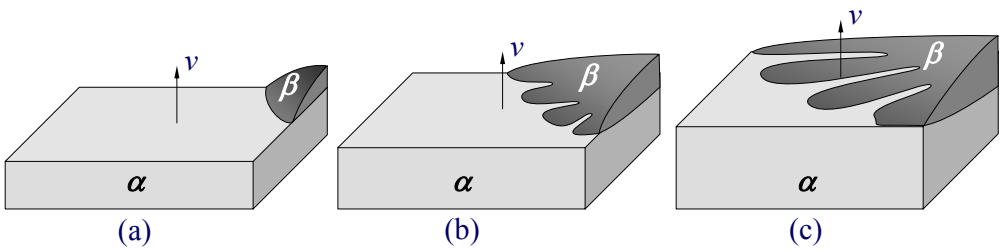

Fig. 3. Schematic of the overlay growth mechanism of one phase (in this case β) over a planar front of α. (From [13,23]).

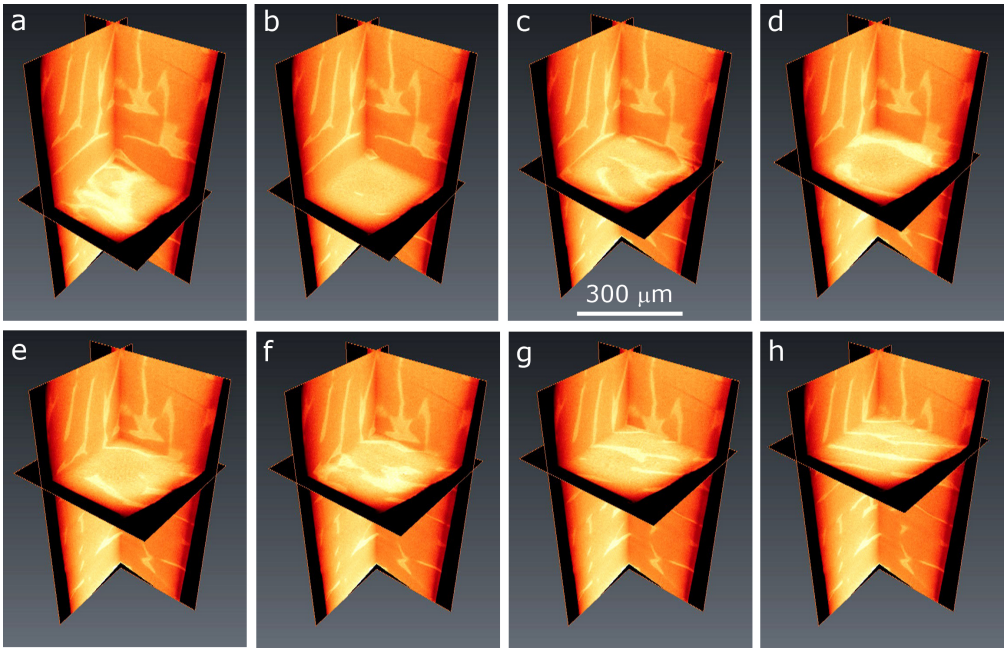

Fig. 4. 3D reconstructured X-ray tomography views of the α (dark brown) and β (brown-yellow) microstructure in a region of the specimen shown in Fig. 2, where bands (in (b)) are destabilized and give rise to a lamellae structure (in (h)). The thermal gradient G is vertical and up.

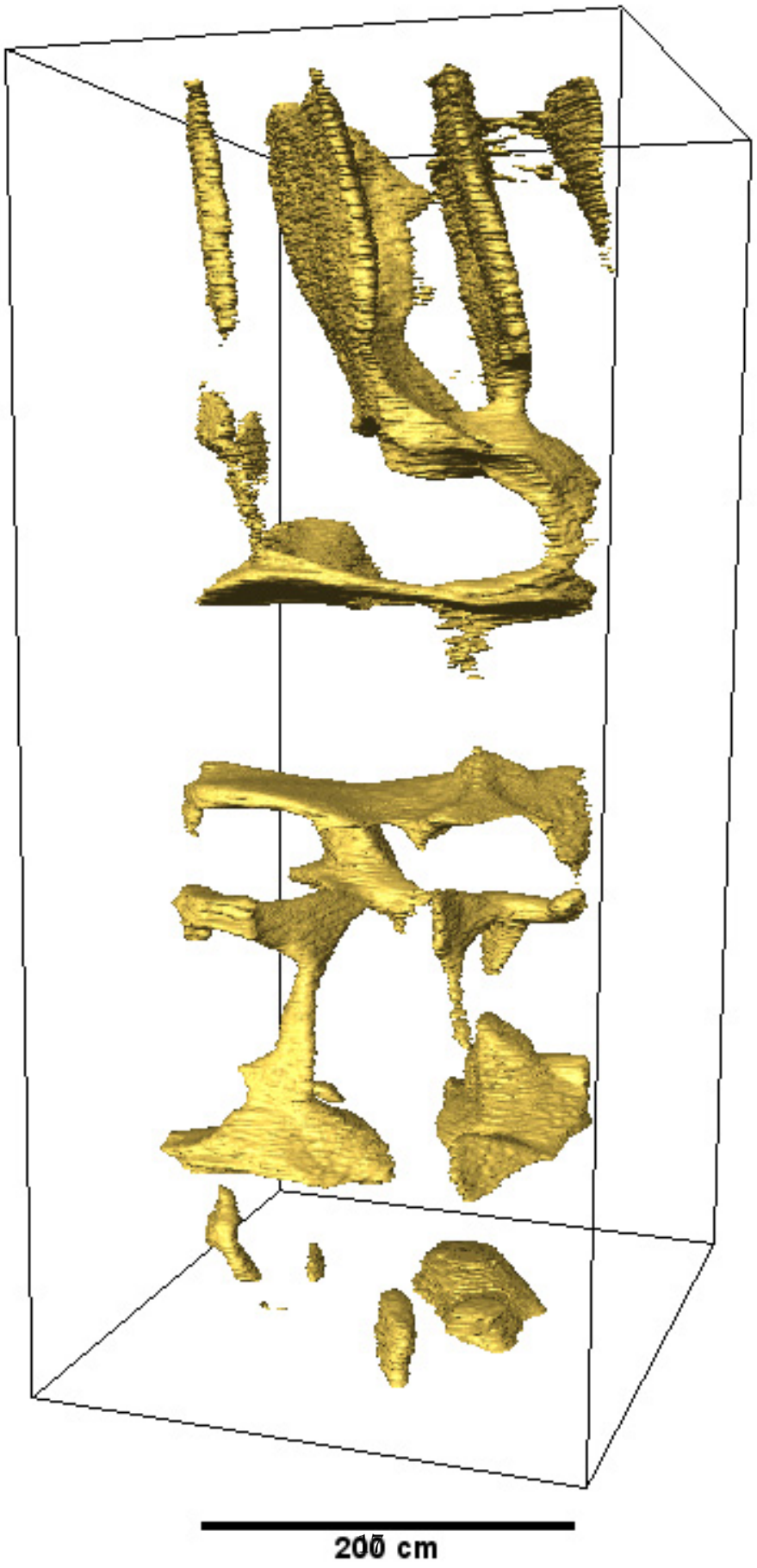

Fig. 5. 3D segmented view of the β phase in a region of the specimen shown in Fig. 2. The transition from lamellae to bands is evident. The thermal gradient G vertical and up.